SEMARAK ILMU PUBLISHING

Journal of Advanced Research in Fluid Mechanics and Thermal Sciences

Journal homepage:
https://semarakilmu.com.my/journals/index.php/fluid_mechanics_thermal_sciences/index
ISSN: 2289-7879

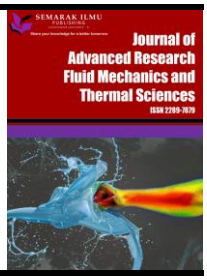

Thermoelectric Energy Harvesting from the Roof and Attics of a Building

Saleh Umar Abubakar[1,*], Siti Amely Jumaat[2], Babangida Yakubu[3], Yau Shuaibu Haruna[4], Suleiman Abdulrahman[1]

[1] Centre for Atmospheric Research, National Space Research and Development Agency, Kogi State University Campus, Anyigba, Nigeria
[2] Department of Electrical Engineering, Faculty of Engineering and Electronic Engineering, Universiti Tun Hussein Onn Malaysia, Malaysia
[3] Department of Electrical Engineering, Federal Polytechnic Mubi, Adamawa State, Nigeria
[4] Department of Electrical and Electronic Engineering, Abubakar Tafawa Balewa University, Bauchi, Nigeria

ARTICLE INFO

Article history:
Received 10 October 2023
Received in revised form 26 February 2024
Accepted 7 March 2024
Available online 30 March 2024

Keywords:
Thermoelectric Generator (TEG); national instrument; heatsink; rooftop; attic area; harvesting

ABSTRACT

Globally people are faced with difficulties in environmental pollution, increasing power costs, and global warming. As such researchers are focusing on enhancing energy-harvesting using thermoelectric generators for power generation to lessen the difficulties. Through the Seebeck effect, thermoelectric generators (TEGs) have proven their ability to convert thermal energy into electric power. Given the unique benefits they present, thermoelectric generators have arisen in the recent decade as a possible alternative to other green power generation technologies. A thermoelectric generator (TEG) is a solid-state device that converts thermal energy into electrical energy. TEG consists of elements of p and n-type semiconductors, connected thermally in parallel and electrically in series. In this paper, one hundred and ninety-two thermoelectric generators connected in series and parallel were used to investigate the thermal energy potential at the roof and attic area for domestic application for 20 days from the falling solar radiation on a residential prototype in Bashar, Wase Local government area of Plateau State. A theoretical analysis was used in determining the average output power (P) due to the delta T across the thermoelectric generator module junction. The load resistance value of the thermoelectric generator configuration was evaluated. The results show that the TEG generated power output ranging from 217 mW to 1.99 W throughout the day, 5.97 mW to 13.8 mW in the morning, and 6.8 mW to 36.9 mW in the evening. Furthermore, The finding also reveals that the attic side has the capacity to store thermal energy, which can be harnessed owing to the fast heat transfer to the surroundings during the convection process. In conclusion, solar irradiance has a major impact on the system.

1. Introduction

The human population in Nigeria has increased for over a decade. This brings about a substantial rise in residential housing in urban and rural areas due to population growth. A study conducted by Akbari *et al*., [1] indicates that over 60% of these residential houses are covered with roofs. In addition, rising urban surface temperatures depend on these population growths within a decade,

* *Corresponding author.*
E-mail address: abubakarumarsaleh1982@gmail.com

https://doi.org/10.37934/arfmts.115.2.8395

thus, creating the urban heat island. Urban heat islands arising from the thermal behaviour of different urban surfaces contribute to heat stress, climate change, and global warming [2].

This is because surface materials with low albedo absorb more thermal energy, including both aspects. First, the property of impervious surfaces, namely roads, streets, roofs, and walls, prevents heat dissipation by evaporation. Therefore, improving the ability to absorb solar energy. As a result, the stored and absorbed heat is released to the environment as sensible heat at night, causing a high-temperature difference on the surface. Secondly, the roof is the most dominant heating element in the urban environment due to daytime solar radiation.

Bashar town is exposed to high temperatures of 22°C to 36°C due to increased solar radiation and high humidity. Located 9°N and 10°E from the equator, Bashar falls into a tropical climate with an average solar radiation level of 5.24 kWh/m2 to 6.43 kWh/m2 in a year [3]. There are about 7 hours of sunlight every day, and the hottest hours are between 11:30 am and 4:30 pm [4]. Figure 1 depicts the level of solar radiation in a day. Studies at a residential house in Bashar show that 76% of solar heat comes from the roof [5].

In addition, the roof surface absorbed 20% to 90% of the radiation at 1 kWh / m2 of solar radiation in clear weather [6,7]. Furthermore, the heat transferred from the roof surface is trapped in the attic. Thus creating a higher ambient temperature between these two surfaces. Therefore, a large amount of heat energy can be used and converted into electrical energy [8-11]. However, the system is bulky and unsuitable for domestic implementation concerning the consumer roof-mounted application as obtained in the previous studies [12-15].

Yoo-Suk *et al*., [16] conducted a thermoelectric energy harvesting from a temperature gradient on a building through a stationary model, in the model, the time domain accounts for the transient behavior of the TEG. The results indicate that 70 mJ was generated. In addition, Qiliang *et al*., [17] designed a thermoelectric-powered wireless sensor network platform for smart buildings using an energy equilibrium algorithm. The findings revealed 0.42 mW of power was produced under a sampling time of 2 has conducted by Fathabadi [18].

The method described in this study focuses on the simple configuration of the TEG on the roof of a metal shingle to investigate and evaluate the thermal energy potential. The paper also shows the ability to convert heat energy into electrical energy from solar radiation on the roof and attic areas. The effect on TEG output power in both configurations has been observed. The next section describes a theoretical thermoelectric generator followed by the experimental setup. Finally, the research findings are discussed and presented.

2. Thermoelectric Generator

The TEG module operates according to the Seebeck effect (α), which converts thermal energy directly into electrical energy [19-21]. The TEG configuration consists of multiple TEGs coupled to the circuit [22]. The configuration setup is a series and parallel combination to achieve the desired current and voltage depending on the load requirements. Figure 1 shows the schematic of the TEG module. Solar radiation provides the heat source for the hot junction, QH is the thermal energy at the hot junction, the cold junction disperses the heat, and the QL is released into the surrounding air. Furthermore, the internal resistance of the TEG is taken as Rin.

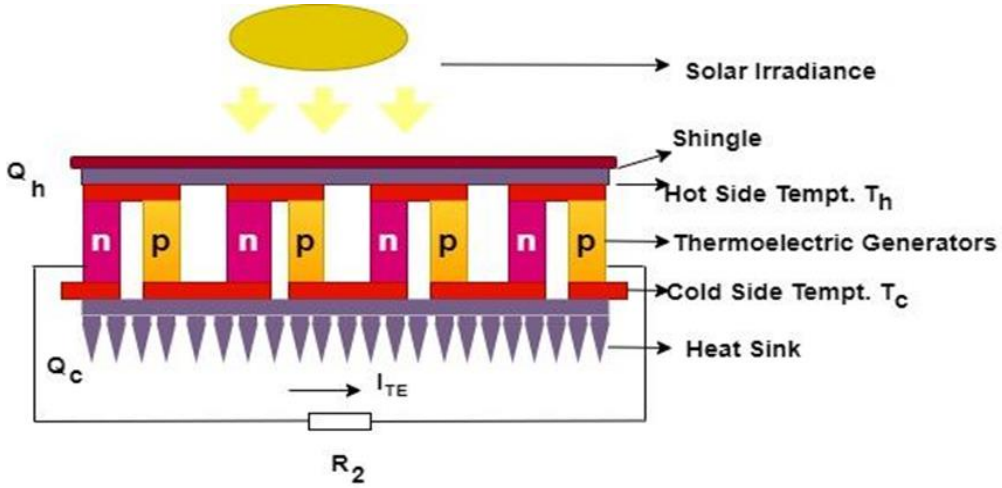

Fig. 1. Schematic diagram of heat flux distribution for a single TEG module

The thermal energy equation for the hot junction is given in Eq. (1), and the thermal energy at the cold junction is obtained using Eq. (2) [23].

$$\mathbb{Q}_{\mathrm{H}} = \alpha \mathrm{T_H I} + (\lambda\, \mathrm{A} / \mathbb{L})\Delta \mathrm{T} - 0.5\, l^2 R_m \tag{1}$$

$$\mathbb{Q}_{\mathrm{L}} = \alpha \mathrm{T}_L \mathrm{I} + (\lambda\, \mathrm{A} / \mathbb{L})\Delta \mathrm{T} - 0.5\, l^2 R_m \tag{2}$$

where T_H is the hot junction temperature, T_L is the cold junction temperature, A is the surface area, L is the length λ is the thermal conductivity, and ΔT is the delta T. The waste heat at the cold junction determines using Eq. (3).

$$\mathbb{Q}_L = K(T_{old} - T_{ambient}) \tag{3}$$

where T_{cold} and $T_{ambient}$ are the temperature at the cold junction and the ambient, respectively. The current I of the TEG module is obtained using Eq. (4) [23].

$$\mathrm{l} = \mathrm{V}_{DC}/(R_m + R_{eload}) \tag{4}$$

The open-circuit voltage, V_{oc} obtained using Eq. (5)

$$\mathrm{V}_{DC} = \propto \Delta \mathrm{T} \tag{5}$$

where ∝ is seebeck coefficient, R_{eload} is the load resistance. Theoretically, the optimum power output, P_{max}, is computed at the internal resistance, R_{in} of the TEG module, equal to a load resistance, R_{eload} given in Eq. (6).

$$\mathrm{P}_{max} = V_{DC^2}/4R_m \tag{6}$$

The equivalent circuit of the TEG is represented by a voltage in series with internal resistance, as shown in Figure 2. The open-circuit voltage generated by the TEG module is proportional to the temperature difference, but the internal resistance is temperature independent [24].

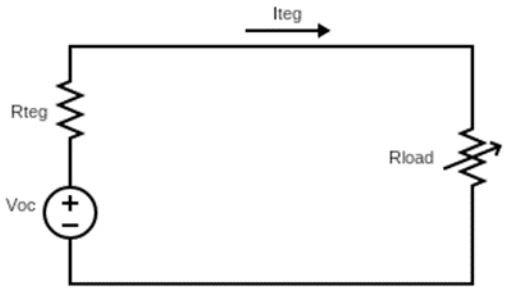

Fig. 2. The interrelation between internal resistances with the load resistance

3. Methodology

Figure 3 shows a real-time experimental setup for temperature measurement of the TEG module. One hundred ninety-two thermoelectric generators (TEGs) with an area of 1 m2 were sandwiched between the metal shingle rooftop materials and the heatsink, and the hot junctions were attached to the metal shingle and the cold junction at the heatsink. In addition, a thin layer of thermal paste is used on the surface of the TEG and heat sink to increase thermal conductivity.

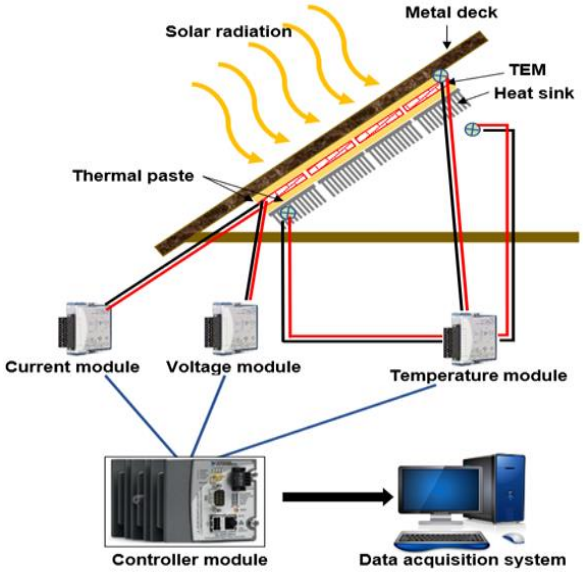

Fig. 3. TEG experimental set-up

The heatsink is used at the cold junction to absorb the heat on the cold junction terminal in order to increase the efficiency of natural wind cooling. Solar Pyranometer is used to measure the amount of solar radiation to study the effect on the amount of heat released on the roof.

A K-type thermocouple was used for the TEG hot-junction temperature measurements, and a heatsink was used to cool the cold-junction temperatures, as shown in Table 1. Another thermocouple was also used to measure the ambient temperature. Temperature data was obtained from the NI-9211 module, the voltage was obtained from the NI-9201 module, and the current was obtained from the NI-9203 module of the national instrument (NI). All the data were recorded at a 1-second update cycle for 24 hours over 20 days. The data were processed using excel. Theoretical calculations using Eq. (1) to Eq. (6) were performed to provide an understanding of the system's thermal and electrical potential using 10% uncertainty values as part of the calculation. Table 1 shows the dimensions of TEG.

Table 1
Properties of type K thermocouples

Temperature range (°F)	Limit of error standard special		EMF (mV) over temperature range
-300 to 32	±2%	N/A	
32 to 530	±4°F	±2%	0 to 11.243
530 to 2300	±3/4%	±3/8%	11.243 to 50.990
Melting point (°C)			1430
Electrical resistivity (Ω/CMF @20°C)			425
Thermal conductivity (Watts/cm/°C @100°C)			0.192

Figure 4 illustrate the system output via the Labview interface for different system parameter measurements.

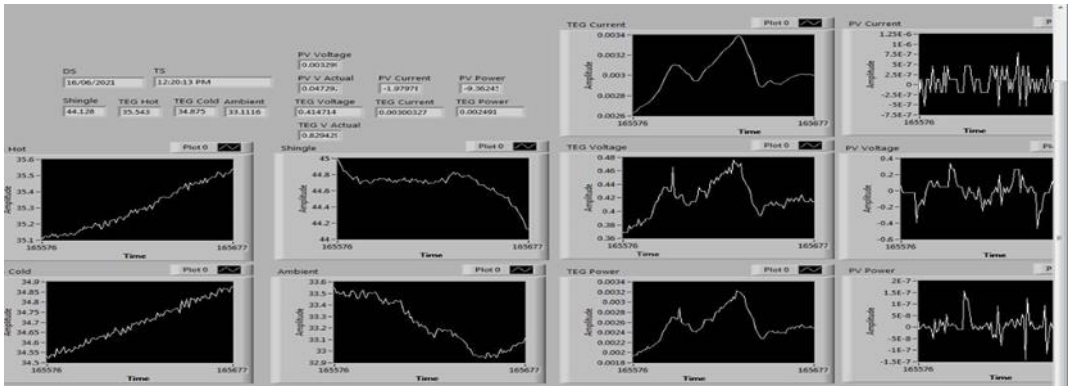

Fig. 4. LabVIEW interface

Before conducting the proper experiments, a preliminary test was carried out to ascertain the power output and resistance properties of two TEGs with the characteristics listed in Table 2. This test involved connecting the TEGs in series with a rheostat load to obtain the internal resistance of the TEG. Figure 5 shows serial and parallel TEG topologies for simulation purposes. In order to determine the total internal resistance, several combinations are made by changing the connection.

Table 2
Thermoelectric generator [25]

Description	Parameter
Type	TEC1-12706
Cold temperature, °C	27
Hot temperature, °C	300
Vmax, V	16
Seebeck coefficient, Se (V/K)	0.053
Heat coefficient, Qmax (Watt)	61
Electrical resistance, Reg (Ω)	2.57
Temperature gradient, ΔT (°C)	70
The quality factor, X	0.930
Thermal resistance, RQ (°K/W)	1.952
A figure of merit, ZT	0.701

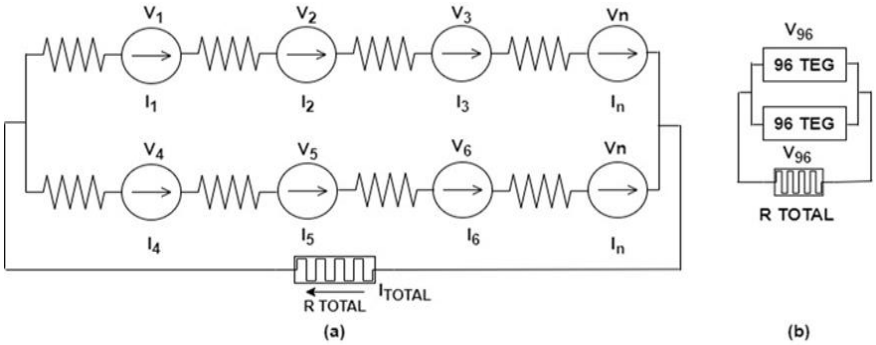

Fig. 5. The TEG configuration for (a) series (b) parallel

The experiments were conducted under real atmospheric conditions to achieve the real-time temperature characteristic of the TEG. The temperature spectrum for hot junction temperatures is 30°C to 55°C. Whereas the cold junction is connected to the heat sink and provides natural cooling. After that, the data was logged for 30 minutes. According to the thermocouple specifications, the uncertainty of the utilized thermocouple is ±16.7% °C. The National Instrument module's structure is comparable to the widespread application of TEG in real-time observations. The power output of the different load resistances is shown in Figure 6.

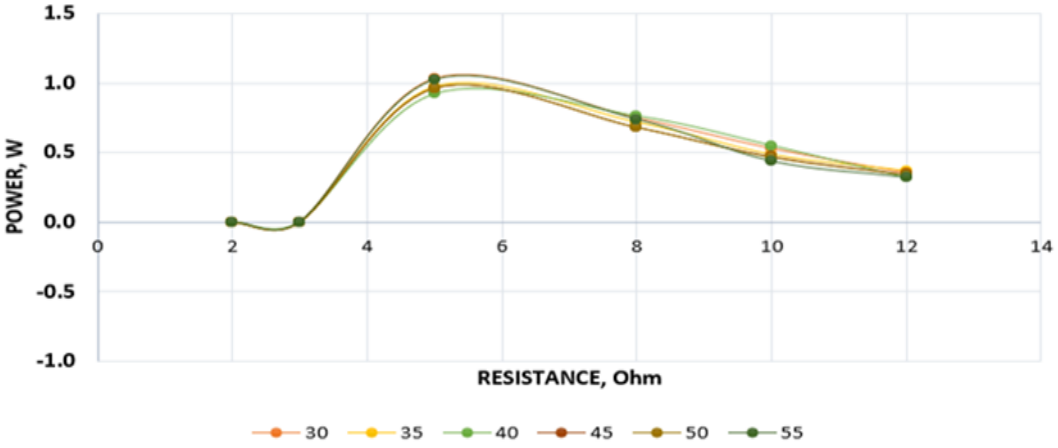

Fig. 6. Power output for different resistance

4. Result and Discussion

4.1 Temperature Behaviours during the Experiment

Figure 7 shows the 24-hour temperature measurements as a direct function of solar radiation and environmental evolution. Therefore, the data is monitored and logged with a temperature variation per second for an update cycle in the investigation. The temperature of both the hot and cold junctions as well as the ambient are taken into consideration while assessing the thermal energy of the TEG's performance. The measurements were divided into three times of the day, morning time (12:00 to 6:00 am), day (6:00 am to 6:00 pm), and evening (6:00 pm to 12:00 am). The division was to achieve a broad investigation and analysis of the temperature potential at the roof and attic area of the building. The highest temperature was achieved during the daytime (6:00 am to 6:00 pm) as compared to the morning and evening time. In the evening and morning time, the temperature drips gradually as a results of the low amount of solar irradiance on the roof. Remarkably, thermal energy was still obtainable owing to the capability of the roofing shingle to supply the solar irradiance to the environment. This allows the use of TEG to generate heat energy from the attic.

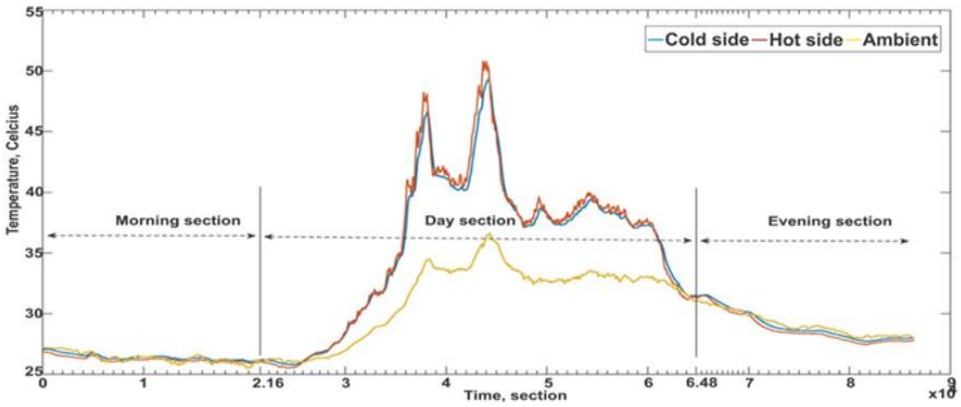

Fig. 7. Temperature variation

Figure 8 shows the delta T (ΔT) analysis. The maximum delta was 0.3433°C to 0.4881°C, while the minimum was 0.1986°C to 0°C. Conversely, the average was between 0.1988°C and 0.3685°C. It points out that the ability of roofing shingles to store thermal energy generates the inexhaustible potential for harvesting thermal energy with or without solar radiation both day and night.

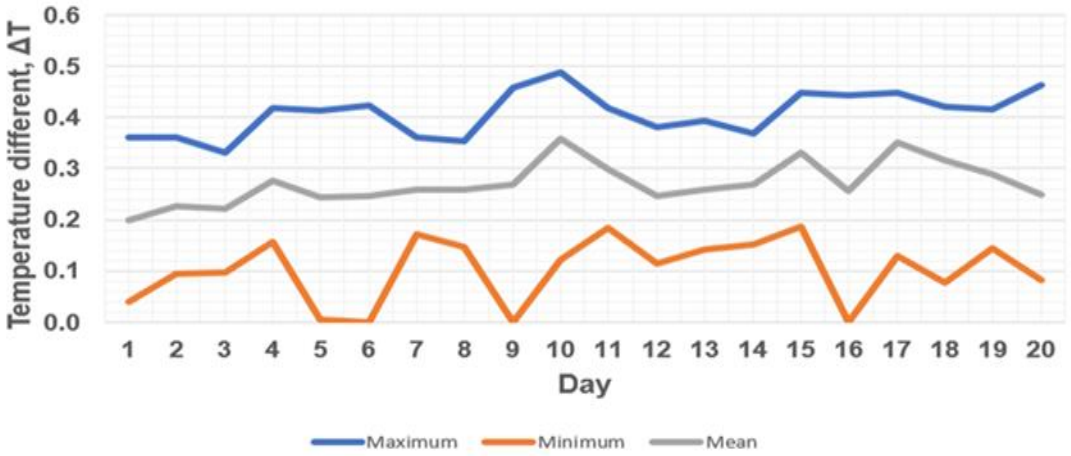

Fig. 8. Delta T at morning time

The experiment's temperatures are influenced by good weather behaviors, this correspond to the findings obtained in the previous studies [26-30], this is seen on the 2nd, 6th, and 9th days as seen in Figure 9. The highest temperature is between 0.7932°C and 0.3523°C in the evening. In addition, the average temperature is 0.3943°C to 0.2934°C, and the lowest temperature is 0.1979°C. Consequently, the system can attain a 50% increase in the daytime as compared to the morning time.

The highest daytime delta T was between 2.2°C and 6.181°C. The average temperature is between 0.3121°C and 0.9781°C, the lowest temperature was at 0°C, as shown in Figure 10.

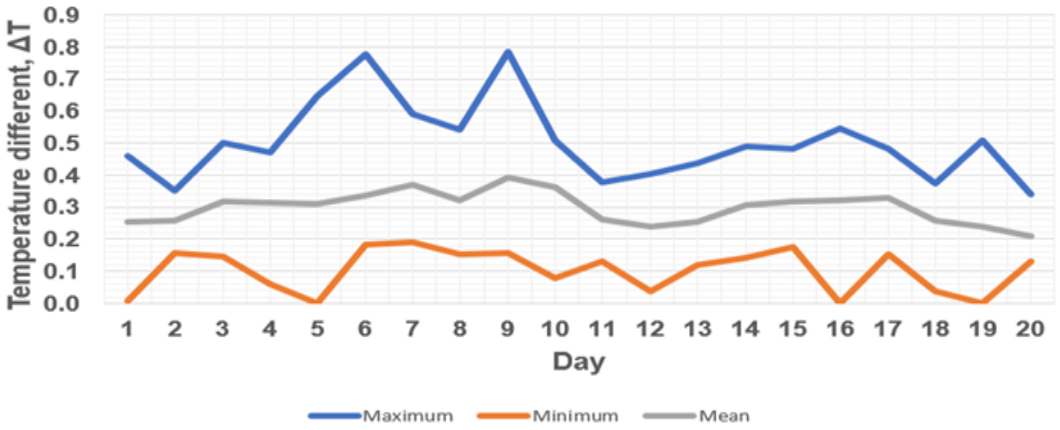

Fig. 9. Delta T for the evening section

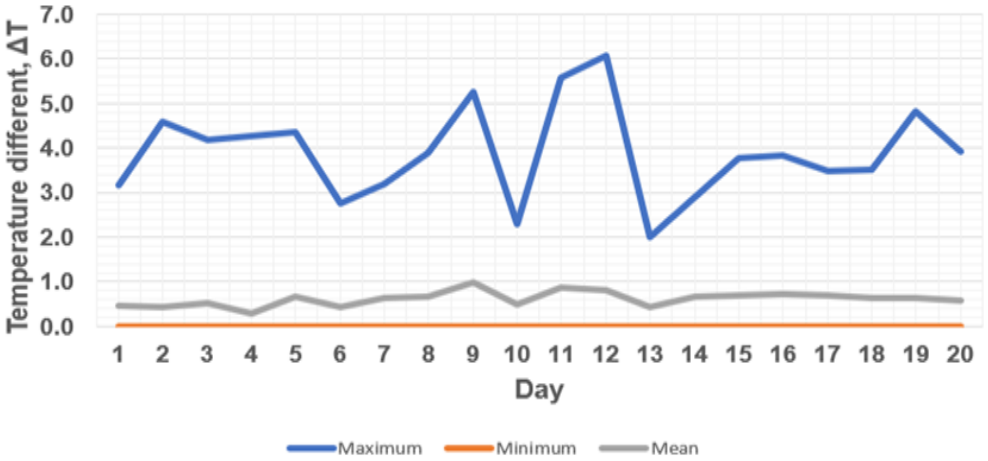

Fig. 10. Delta T for the day section

According to the temperature result, high-intensity polarization change takes place on the TEG module's hot and cold junctions. As a result, the distribution of temperatures has been divided into three portions for additional investigation and to minimize simulation errors for the TEG module's potential energy generation. Based on the theoretical approach, a negative value is the anticipated outcome. Numerous factors, including humidity, rain, haze, and partial solar irradiance shading could affect the outcome of this investigation. Thus, as previously stated, the roof's temperature is influenced by the environment.

The overall temperature variation of the day indicates that it is likely to harvest electrical energy potential from the heat of solar irradiance. Nevertheless, in order to increase the rate of achievement in terms of the potential delta T on both sides of the TEG module, the efficiency of the TEG configuration must be evaluated prior to being mounted.

In addition, the temperature difference measured on the roof is essential because the energy produced by the TEG module depends on the delta T (ΔT). Hence, using TEG simulation and proper realization of renewable energy will assist determine the energy generated via the current temperature distribution. Typically, output power, voltage, and current are used to assess performance in TEG systems.

4.2 Potential Power Evaluation

The TEG electrical power potential evaluation in relation to solar radiation was conducted. Taking into account the experimental temperature for the hot and cold junctions of the TEG, the voltage generated was computed using Equation 5. The TEG internal resistance and the Seebeck coefficient are 2.57 Ω and, 53 mV/°K, respectively. The serial and parallel connections used in the proposed TEG array designs were found in Husainy *et al.*, [26]. The system achieved the highest power transfer once the TEG internal resistance matched the load. As a result, the overall internal resistance of the TEG design is 135.95 Ω in parallel and 511.97 Ω in series.

Figure 11 depicts the output power generated during the morning and evening time. From day 6 to day 9, evening power generation increased by 66% as compared to morning power generation. The lowest and highest power generated were 6.76mW and 33.9mW in the evening, respectively. In the morning time, the highest power ranges from 5.96mW to 12.8mW. Furthermore, for both TEG designs, the mean power over 20 days is 9.21 mW in the morning and 14.5 mW in the evening

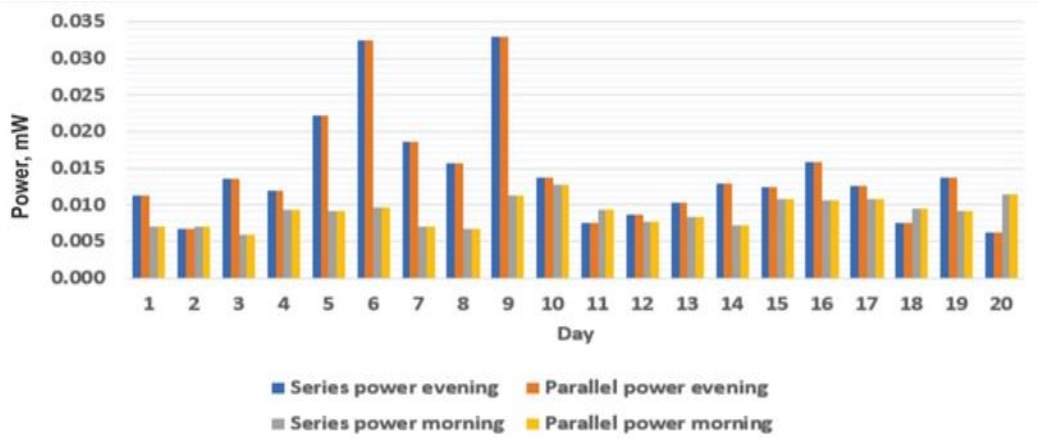

Fig. 11. Output power for the morning and evening time

Figure 12 concentrates on days 6–9, where the parallel current is 66% larger than the series current at both times. The highest parallel and series currents are 16.4mA and 8.11mA in the evening. In the morning, the current is 5.21 mA for connections in series and 11.2 mA for connections in parallel. The lowest current, in comparison, is 3.55 mA in series and 7.06 mA in parallel in the evening. In the morning, the lowest current for connections in parallel is 6.93 mA, and 3.44 mA for connections in series.

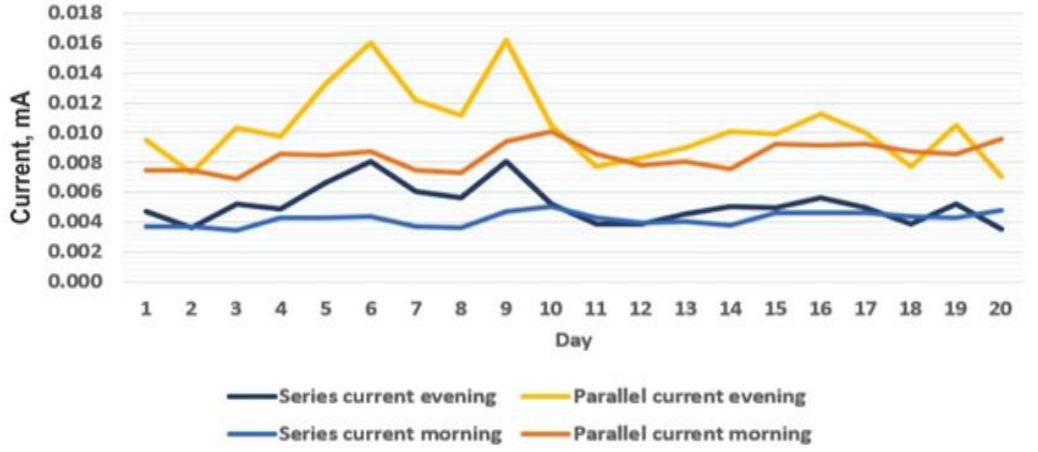

Fig. 12. Current for the morning and evening section

The voltages obtained in Figure 13 for the two TEG setups followed the same trend as the currents in Figure 12 in the morning and evening. Nevertheless, the series arrangement offers a better voltage with a 66% improvement over the parallel arrangement. The morning voltages of the series connections are therefore 2.62V and 1.82V, respectively, for the highest and lowest voltages. In addition, the highest and lowest voltages for the parallel connection in the morning are 1.28V and 0.87V, respectively. In the evening, 4.08V and 1.79V, respectively, are the highest and lowest values for the series connections.

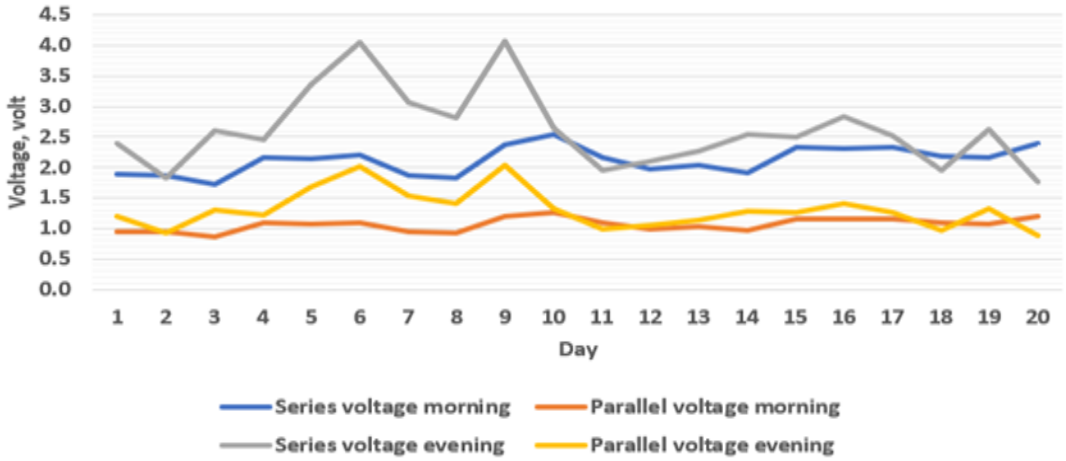

Fig. 13. Voltage for the morning and evening *time*

As revealed in Figure 14, the solar irradiance effect considerably enhances the power generation in the two TEG setups, increasing by 99.45% and 97.3% at optimum and minimum, respectively, as compared to the morning time. On the other hand, during the evening hours, the highest and lowest values respectively increased by 98.5% and 96.9%. The pattern is the same in the two designs, with an optimal daytime value of 1.99 W and a minimum of 217 mW. The findings indicate that solar radiation's impacts have a direct effect on the rise in roof temperature.

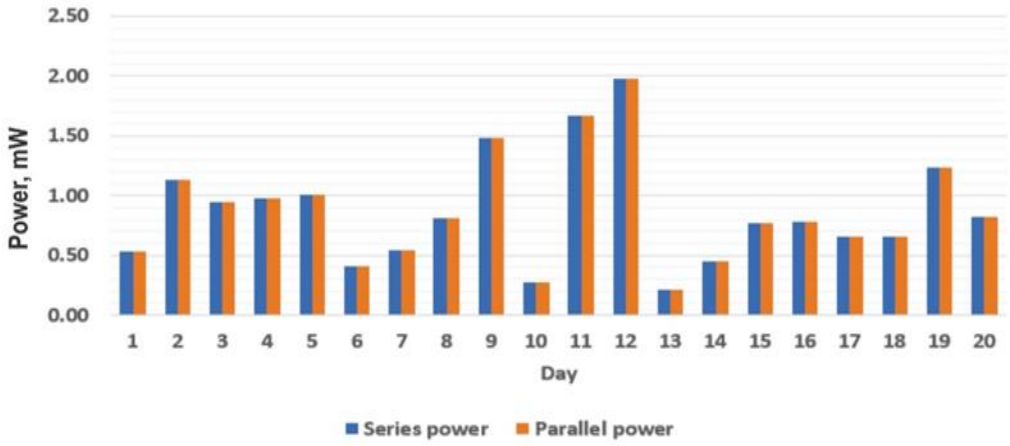

Fig. 14. Output power for the day section

The current variations can be seen in Figure 15 for both parallel and series setups. With the highest and lowest current values of 126 mA and 41.6 mA, respectively, the results show a 49.5% increase for parallel in comparison to the series. Additionally, 63.5mA and 21.6mA are the series' highest and lowest values of the current, respectively.

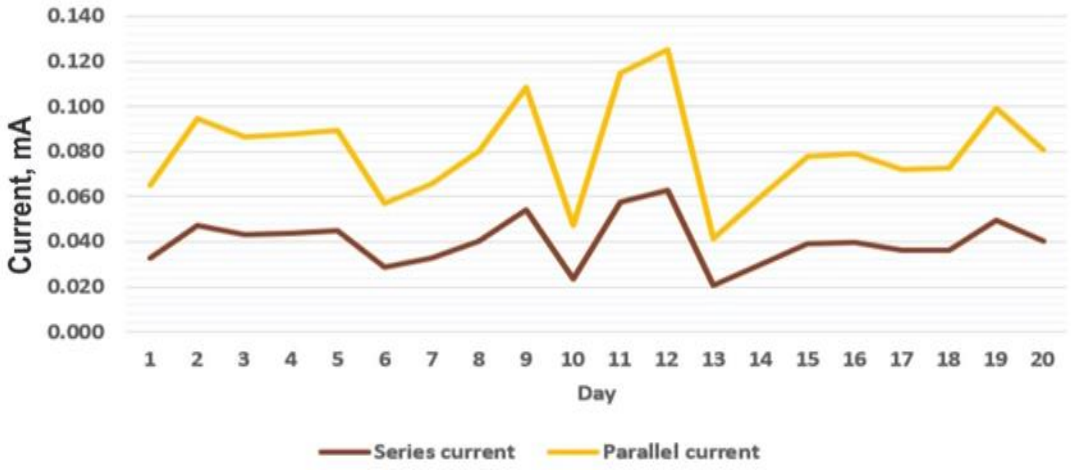

Fig. 15. Current for day section

Figure 16 depicts the voltage variation for the daytime. Essentially, the series setup produced a better voltage than the parallel setup and has a 49.86 % increase. In comparison to parallel setups, which obtained 15.9V and 5.30V, respectively, series setups achieved 31.7V and 10.6V as their highest and lowest voltages.

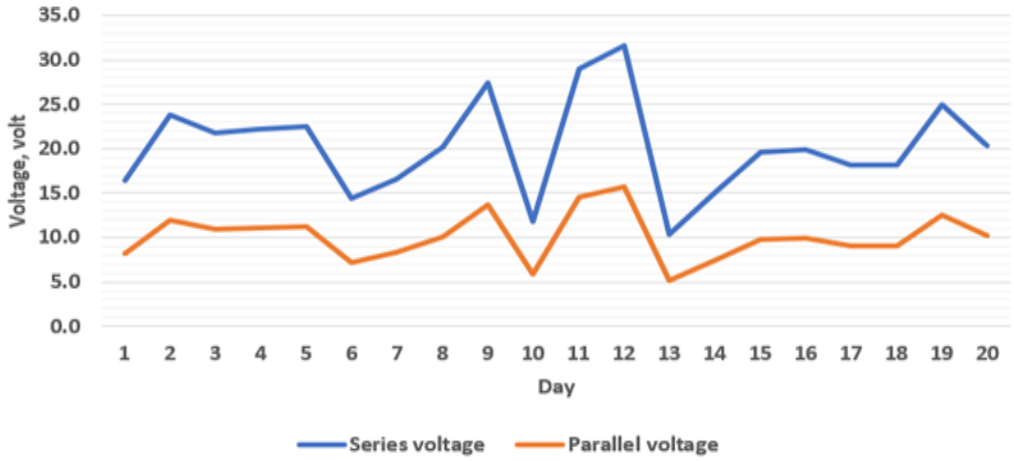

Fig. 16. Voltage for day section

5. Conclusion

The present research analyzed the 20-day solar radiation's thermal potential on roofs and attics. From the result, thermal energy has been shown to be significantly impacted by solar radiation. A substantial delta T measured at the TEG module shows that the morning had the lowest daily delta, T, proceeded by the evening, and the day had the highest delta T. In the morning and evening, the attic's thermal energy is higher than that of the roof. As a result, it switches the TEG module's orientation from hot to cold. This process is comparable to how polarity changes produce electrical energy. The highest delta T values were in the morning (0.4871 °C), evening (0.7842 °C), and daytime (6 °C).

Additionally, it was discovered that both configurations of the TEG module's output power were comparable. On the other hand, the voltage produced shows that the parallel configuration is less as compared to the series arrangement. While we notice a reverse tendency for measurements of current, where the parallel setup can attain 65% higher than the series. The TEG's output power ranged from 1.99 W to 216 mW during the day, while only 12.9 mW to 5.94 mW and 36.9 mW to 6.8

mW were generated in the morning and evening, respectively. The thermal energy reaching the roof throughout the day is thus impacted by the total amount of solar irradiation. Furthermore, even when only a small quantity of electricity is produced, thermal energy from the roof's attic area is useful. More energy can be generated from the roof and attics area by using light colour materials, adding more insulation, and a radiant barrier at the same optimizing the TEG figure of meric.

Acknowledgment
This research was supported by a grant from Universiti Tun Hussien Onn Malaysia (UTHM) through Tier 1 (vot Q366).

References

[1] Akbari, Hashem, S. Menon, and A. Rosenfeld. "White roofs cool the world, directly offset CO_2 and delay global warming." *Research Highlights LBNL Heat Island Group* (2008): 1-2.

[2] Lee, Yee Yong, Mohd Fadhil Md Din, Kenzo Iwao, Yeong Huei Lee, and Nickholas Anting. "Impact of thermal behaviour of different environmental conditions on ambient environment and thermal discomfort in Malaysia." *Indoor and built environment* 30, no. 4 (2021): 520-534. https://doi.org/10.1177/1420326X19897956

[3] Mohd Shatar, Nursyahirah, Mohd Azizi Abdul Rahman, Mohd Nabil Muhtazaruddin, Sheikh Ahmad Zaki Shaikh Salim, Baljit Singh, Firdaus Muhammad-Sukki, Nurul Aini Bani, Ahmad Shakir Mohd Saudi, and Jorge Alfredo Ardila-Rey. "Performance evaluation of unconcentrated photovoltaic-thermoelectric generator hybrid system under tropical climate." *Sustainability* 11, no. 22 (2019): 6192. https://doi.org/10.3390/su11226192

[4] Nasir, M. Ahmad, C. H. Lim, and A. F. Abdullah. "Survey on the empirical method to evaluate the thermal performance of roof assembly." In *Journal of Physics: Conference Series*, vol. 1358, no. 1, p. 012040. IOP Publishing, 2019. https://doi.org/10.1088/1742-6596/1358/1/012040

[5] Suehrcke, Harry, Eric L. Peterson, and Neville Selby. "Effect of roof solar reflectance on the building heat gain in a hot climate." *Energy and Buildings* 40, no. 12 (2008): 2224-2235. https://doi.org/10.1016/j.enbuild.2008.06.015

[6] Rehman, Naveed ur, and Mubashir Ali Siddiqui. "Theoretical and field experimental investigation of an arrayed solar thermoelectric flat-plate generator." *Journal of Electronic Materials* 47 (2018):4742-4756. https://doi.org/10.1007/s11664-018-6363-x

[7] Champier, Daniel. "Thermoelectric generators: A review of applications." *Energy conversion and management* 140 (2017): 167-181. https://doi.org/10.1016/j.enconman.2017.02.070

[8] Shittu, Samson, Guiqiang Li, Xin Tang, Xudong Zhao, Xiaoli Ma, and Ali Badiei. "Analysis of thermoelectric geometry in a concentrated photovoltaic-thermoelectric under varying weather conditions." *Energy* 202 (2020): 117742. https://doi.org/10.1016/j.energy.2020.117742

[9] Nia, M. Hasan, A. Abbas Nejad, A. M. Goudarzi, M. Valizadeh, and P. Samadian. "Cogeneration solar system using thermoelectric module and fresnel lens." *Energy Conversion and Management* 84 (2014): 305-310. https://doi.org/10.1016/j.enconman.2014.04.041

[10] Jeyashree, Y., Y. Sukhi, A. Vimala Juliet, S. Lourdu Jame, and S. Indirani. "Concentrated solar thermal energy harvesting using Bi2Te3based thermoelectric generator." *Materials Science in Semiconductor Processing* 107 (2020): 104782. https://doi.org/10.1016/j.mssp.2019.104782

[11] Uddin, Md Shihab, Anas Abdullah Alvi, Md Nayeem Hasan Mallick, Sree Krishna Das, Md Ashraful Islam, and Rajia Sultana. "Performance Evaluation of a Green and Non-Concentrated Solar Thermoelectric Generator System." In *2019 International Conference on Energy and Power Engineering (ICEPE)*, pp. 1-4. IEEE, 2019. https://doi.org/10.1039/C2EE22248E

[12] Shen, Haishan, Hoojeong Lee, and Seungwoo Han. "Optimization and fabrication of a planar thermoelectric generator for a high-performance solar thermoelectric generator." *Current Applied Physics* 22 (2021): 6-13. https://doi.org/10.1016/j.cap.2020.11.005

[13] Figaj, Rafał, Mateusz Szubel, Estera Przenzak, and Mariusz Filipowicz. "Feasibility of a small-scale hybrid dish/flat-plate solar collector system as a heat source for an absorption cooling unit." *Applied Thermal Engineering* 163 (2019): 114399. https://doi.org/10.1016/j.applthermaleng.2019.114399

[14] Moser, André, Metin Erd, Milos Kostic, Keith Cobry, Michael Kroener, and Peter Woias. "Thermoelectric energy harvesting from transient ambient temperature gradients." *Journal of electronic materials* 41 (2012): 1653-1661. https://doi.org/10.1007/s11664-011-1894-4

[15] Lin, Qiliang, Yi-Chung Chen, Fangliang Chen, Tejav DeGanyar, and Huiming Yin. "Design and experiments of a thermoelectric-powered wireless sensor network platform for smart building envelope." *Applied Energy* 305 (2022): 11779. https://doi.org/10.1016/j.apenergy.2021.117791

[16] Byon, Yoo-Suk, and Jae-Weon Jeong. "Phase change material-integrated thermoelectric energy harvesting block as an independent power source for sensors in buildings." *Renewable and Sustainable Energy Reviews* 128 (2020): 109921. https://doi.org/10.1016/j.rser.2020.109921

[17] Faddouli, A., H. A. M. R. Labrim, S. A. L. A. H. Fadili, B. O. U. C. H. A. İ. B. Hartiti, A. Habchi, M. Ertugrul, B. Cavusoglu, and E. S. İ. D. O. R. Ntsoenzok. "Feasibility and performance investigation of a new smart system integrating planar/tubular thermoelectric generators with solar flat plate collector." *Energy conversion and management* 199 (2019): 111980. https://doi.org/10.1016/j.enconman.2019.111980

[18] Fathabadi, Hassan. "Novel solar-powered photovoltaic/thermoelectric hybrid power source." *Renewable Energy* 146 (2020): 426-434. https://doi.org/10.1016/j.renene.2019.06.141

[19] He, Wei, Gan Zhang, Guiqiang Li, and Jie Ji. "Analysis and discussion on the impact of non-uniform input heat flux on thermoelectric generator array." *Energy conversion and management* 98 (2015): 268-274. https://doi.org/10.1016/j.enconman.2015.04.006

[20] Negash, Assmelash A., Tae Young Kim, and Gyubaek Cho. "Effect of electrical array configuration of thermoelectric modules on waste heat recovery of thermoelectric generator." *Sensors and Actuators A: Physical* 260 (2017): 212-219. https://doi.org/10.1016/j.sna.2017.04.016

[21] Saleh, Umar Abubakakar, Siti Amely Jumaat, Johar Muhammad Akmal, and Wan Akashah Wan Jamuludin. "The real-time Monitoring of TEG using the LabVIEW Technique for Green Energy Generation." *Multidisciplinary Applied Research and Innovation* 2, no. 3 (2021): 112-116. https://doi.org/10.30880/mari.2021.02.03.022

[22] Saleh, Umar Abubakar, Muhammad Akmal Johar, Siti Amely Binti Jumaat, Muhammad Nazri Rejab, and Wan Akashah Wan Jamaludin. "Evaluation of a PV-TEG hybrid system configuration for an improved energy output: a review." *International Journal of Renewable Energy Development* 10, no. 2 (2021): 385-400. https://doi.org/10.14710/ijred.2021.33917

[23] Adedoja, Oluwaseye Samson, Umar Abubakar Saleh, Adeyemi Raifu Alesinloye, Tebe-Ebi Justice Timiyo, Ifeanyi Francis Onuigbo, Olalekan Opeyemi Adejuwon, and Ezekiel Josiah. "An energy balance and multicriterial approach for the sizing of a hybrid renewable energy system with hydrogen storage." *e-Prime-Advances in Electrical Engineering, Electronics and Energy* 4 (2023): 100146. https://doi.org/10.1016/j.prime.2023.100146

[24] ALLDATASHEETCOM, P. "Thermoelectric Cooler Performance Specifications. Performance curves." *HB. Rev* 2, no. 3 (2018): 541.

[25] Husainy, Muhamad Fakhrul Amr, Muhammad Afiq Mohamad Rosli, Muhd Zul Syafiq Norizan, Nur Hidayah Saifullah Arifin, Nur Qistina Eiman Mahathir, Umar Abubakar Saleh, and Siti Amely Jumaat. "Solar thermoelectric generator (STEG) for lighting system." *Evolution in Electrical and Electronic Engineering* 2, no. 2 (2021): 811-818. https://doi.org/10.30880/eeee.2021.02.02.097

[26] Khang, Wong Chin, Siti Amely Jumaat, Muhammad Akmal Johar, and Umar Saleh Abu Bakar. "Development of Prototype Hybrid Photovoltaic-Thermoelectric (PV-TEG) System." In *2023 IEEE 3rd International Conference in Power Engineering Applications (ICPEA)*, pp. 175-178. IEEE, 2023. https://doi.org/10.1109/ICPEA56918.2023.10093157

[27] Fohimi, Nor Azirah Mohd, Koay Mei Hyie, Siti Shareeda Mohd Nasir, Norasikin Hussin, and Fairosidi Idrus. "Experimental Study of Indoor Air Temperature in the Laboratory." *Journal of Advanced Research in Experimental Fluid Mechanics and Heat Transfer* 9, no. 1 (2022): 1-8.

[28] Nuruljannah Hussein. "Thermal Performance of Nanofluid in Automobile Radiator." *Journal of Advanced Research Design* 107, no. 1 (2023): 1-15.

[29] Fahmy, M., M. Morsy, H. Abd Elshakour, and A. M. Belal. "Effect of thermal insulation on building thermal comfort and energy consumption in Egypt." *Journal of Advanced Research in Applied Mechanics* 43, no. 1 (2018): 8-19.

[30] Irfan, Muhammad, and Faizir Ramlie. "Analysis of parameters which affects prediction of energy consumption in buildings using Partial Least Square (PLS) approach." *Journal of Advanced Research in Applied Sciences and Engineering Technology* 25, no. 1 (2021): 61-68. https://doi.org/10.37934/araset.25.1.6168